NJC

Accepted Manuscript

This article can be cited before page numbers have been issued, to do this please use: A. A. A. Selvam, L. Chandrasekaran, N. S. Thomas, S. Kuppusamy, T. A. Antony and K. Senthamaraikannan, *New J. Chem.*, 2015, DOI: 10.1039/C5NJ01369K.

ROYAL SOCIETY OF CHEMISTRY

www.rsc.org/njc

View Article Online
DOI: 10.1039/C5NJ01369K

Journal Name

ARTICLE

Synthesis, structure prediction, pharmacokinetic properties, molecular docking and antitumor activities of some novel thiazinone derivatives.

Received 00th January 20xx,
Accepted 00th January 20xx

DOI: 10.1039/x0xx00000x

www.rsc.org/

Selvam Athavan Alias Anand,[a] Chandrasekaran Loganathan,[a] Nisha Susan Thomas,[b] Kuppusamy Saravanan,[a] Antony Therasa Alphonsa[a] and Senthamaraikannan Kabilan*[,a]

A novel series of thiazinone derivatives were obtained from unexpected cyclization of dimethyl acetylenedicarboxylate (DMAD) and diethyl acetylenedicarboxylate (DEAD) with corresponding 3–alkyl–2,6–diarylpiperidin–4one thiosemicarbazones in dry methanol, without catalyst under mild conditions. The structures of newly synthesized compounds were established on the basis of FT–IR, HR–Mass, ^{1}H–NMR, ^{13}C–NMR, ^{1}H–^{1}H COSY, ^{1}H–^{13}C COSY, DEPT–135, and HMBC spectral techniques. From the ^{1}H NMR, all newly synthesized compounds **17**–**24** were found to adopt chair conformation. The theoretical studies were carried out using Schrödinger software suite for the structure prediction, biochemical properties investigation and docking studies of all novel compounds. In order to provide the antitumor activity, all the novel compounds were screened *in vitro* for their cytotoxicity and apoptosis activity against Hep G2 human liver cancer cell line. The biological analysis revealed that the newly synthesized compounds have good/moderate inhibitory activity against the tested cell line.

1. Introduction

Recent advances in biochemistry and medicinal chemistry allow access to do wonders in pharmaceutical applications. To understand the principles of medicinal chemistry, it is necessary to know about the physicochemical properties including possible biological activity of the chemical compounds. Organic compounds being continue to be important in the development of new agents for treating diseases. However, heterocyclic compounds with increasingly specific pharmacological activities are clearly dominant. Even in the field of modern medicinal chemistry, heterocyclic alkaloids like morphine derivatives are the active ingredients in many natural remedies.[1–4] Modifications in drug motifs using heterocycles can also provide favorable biological properties. We are actively doing research in the area of drug discovery and synthesis of novel heterocycles.[5–8] Our research is focused on the design and synthesis of 3–alkyl–2,6–diarylpiperidin–4–ones derivatives with heterocyclic systems such as oxime ethers, thiadiazolines, imidazoles/benzotriazoles, thiones, piperazine, morphine, benzimidazole exhibit diverse biological activities.[9–15]

In the present work, we report the way of reactivity between 3–alkyl–2,6–diarylpiperidin–4–one thiosemicarbazone derivatives and DMAD/DEAD; an electron–deficient alkyne diester which is used as dienophile and / or dipolarophile in cycloaddition reactions.[16–20] The molecular structure of the resulting heterocycles was investigated using spectral techniques and theoretically by HOMO-LUMO energy gap calculations. To understand the fundamental drug–like properties of the newly synthesized compounds, pharmacokinetic properties predictions were carried out based on *Lipinski's rule of five*. The docking studies were performed to find the mode of interactions between the compounds and the selected protein. Both the pharmacokinetic properties predictions and the docking studies were examined using *Maestro v 9.3.5* [21] of Schrödinger software suite, 2012.

The recent anticancer drug research indicates that the piperidinone derivatives exhibit potent and sufficient activity against cancer cell lines.[22] All the newly synthesized molecules were evaluated for their cytotoxicity on human liver cancer cell line Hep G2 through MTT (3-(4,5-dimethylthiazol-2-yl)-2,5-diphenyl tetrazolium bromide, a yellow tetrazole) assay. The apoptotic activity against Hep G2 was also carried out and the morphological studies were performed using Acridine Orange (AO)/Ethidium bromide (EB) staining.

[a] *Drug Discovery Lab, Department of Chemistry, Annamalai University, Annamalainagar, Tamilnadu – 608002, India.*
[b] *Department of Bio-Chemistry and Bio-Technology, Annamalai University, Annamalainagar, Tamilnadu – 608002, India.*
Email: profskabilanau@gmail.com, Tel: +91 94439 24629

Electronic Supplementary Information (ESI) available: [details of any supplementary information available should be included here]. See DOI: 10.1039/x0xx00000x

2. Experimental

2.1. Chemistry

The reaction between thioamides and alkyne diester was widely emphasized for the synthesis of either thiazin–4–ones or thiazolidin–4–ones.[23–28] Thiazinone and thiazolidinone based heterocycles are the most common motifs found in drug design. The derivatives of thiazinone and thiazolidinone are of much interest because of their miscellaneous biological activities such as anticancer,[29] antimicrobial,[30] anticonvulsant,[31] antituberculosis,[32] and anti–HIV.[33] Thiazinone and thiazolidinone derivatives also act as α–Amino–3–hydroxy–5–methyl–4–isoxazolepropionic acid (AMPA) receptor antagonist[34] and inhibitors of bacterial enzyme Mur–B[35] respectively.

The starting material 3–alkyl–2,6–diarylpiperidin–4–ones were prepared in good yields through consecutive steps as reported in the literature.[36,37] The thiosemicarbazone derivatives were prepared in acidic methanol medium by treating thiosemicarbazide with substituted piperidones under reflux condition. These upon recrystallisation in methanol gave pure compounds.[38] The reaction between thiourea/thiosemicarbazone/thioamide derivatives and electron–deficient alkyne diester is the convenient and effective method to synthesize thiazolidinone or thiazinone derivatives. We have considered a trial reaction of 3–alkyl–2,6–diarylpiperidin–4–one thiosemicarbazone derivatives with DMAD/DEAD to investigate in detail about the reactivity.

2.2. Computational Studies

The theoretical calculations reported in this work were performed on a Dell workstation equipped with Xeon processor E3–1225, V2 quardcore, 3.20 GHz personal computer with 8 GB total RAM and with Schrödinger software suite, LLC, New York, 2012.

2.2.1 Identification of Stable Isomer

The quantum chemical calculations of compounds **17** and **25** were performed by using Schrödinger software with *Jaguar*[39] application. The structures of the compounds **17** and **25** were fully optimized in vacuum using density functional theory (DFT) method at B3LYP and M06 hybrid functionals along with 6–31G**, 6–311G**, and 6–311G–3DF–3PD basis sets. Highest occupied molecular orbital (HOMO) energies, lowest unoccupied molecular orbital (LUMO) energies and the energy gap (LUMO-HOMO) of two compounds were calculated and compared. The structure with maximum energy gap was considered as a stable compound.

2.2.2 Pharmacokinetic Properties prediction

The 2D structures of compounds **17–24** were subjected to a computational program using *Qikprop*[40] module of Schrödinger software for the *insilico* determination of pharmacokinetic properties. A preliminary test of the drug–likeness of the compounds was calculated in accordance with *Lipinski's rule of five*.[41] To obey the *Lipinski's rule of five*, the compounds requires molecular weight (mol_MW) of less than 500 amu, no more than 5 and 10 hydrogen bond donors (Donor HB) and hydrogen bond acceptors (Accpt HB) respectively, and the partition coefficient between octanol and water (QPlogPo/w) be less than 5. The compounds which have more than one violation of these rules are not considered as orally active molecule. The properties such as percentage of human oral absorption, aqueous solubility, IC_{50} value for blockage of HERG K+ channels and blood brain barrier permeability were also predicted to know about the basic bioactivity of the compounds.

2.2.3 Docking Studies

The critical interactions between Murine double minutes (MDM2) and p53 proteins have been proved as a promising target for anticancer therapy.[42] The MDM2 is considered as bonafide oncogene, which suppresses the significant activity of the natural tumor suppressor p53. It was observed that the growth of cancer cells was arrested by inhibiting the over expression of MDM2 which demonstrate the significant activation of p53.[43] The 3D co–ordinates of crystallographic structure of MDM2 protein complex[44] (PDB ID: 4ODE) was downloaded from Brookheaven protein Data Bank (www.rscb.com). The protein complex was pre–processed and prepared by *Protein Preparation Wizard*[45] in Maestro of Schrödinger software. The minimization of the complex was continued using OPLS–2005 (Optimized Potential for Liquid Simulations) force field[46] until the root mean square deviation (RMSD) reached the value of 0.3 Å.

The 2D structures of compounds **17-24** were imported from the project table and the structures were minimized and geometrically refined using *Ligprep*[47] module. Conformers were generated using torsional search method with distance dependent dielectric solvation treatment and OPLS–2005 force field. The extra precision (XP) mode of docking was used to find the best fit molecules in the active site of MDM2 protein using *Glide*[48] application of Schrödinger software suite.

2.3. Biological Studies

2.3.1 Cytotoxicity

Human hepatoma cell line, Hep G2 were obtained from the National Centre for Cell Science, Pune, India. The cytotoxic effect of the synthesized compounds **17-24** on Hep G2 liver cancer cell line was evaluated through MTT dye reduction assay as described earlier.[49] The tested compounds were dissolved quantitatively in dimethylsulfoxide (DMSO, Sigma, USA) and diluted to make stock solution. Hep G2 cells were seeded at a density of 5 x 10^3 cells/well into 96 well plates. After 24 h, the cells were treated with various concentrations of the compounds **17-24** in the range of 10-100 µM and incubated for 24 h and 48 h as indicated. The cells were then assayed by the addition of 20 µL of MTT (5 mg/mL in phosphate-buffered saline) per well and incubated in dark at 37°C for 3 h. The purple formazan crystals formed after 3 h were dissolved in 100 µL of DMSO after aspirating the MTT and incubated for further 10 minutes. The mitochondrial dehydrogenase in viable cells that reduces MTT to blue formazan product was measured at 570 nm (measurement) and 630 nm (reference) using a 96 wells plate reader (Bio-Rad, Hercules, CA, USA). Data were collected from six independent experiments and used to calculate the respective means. The

percentage of inhibition was calculated from the data, using the formula:

[(Mean absorbance of treated cells)/(Mean absorbance of sham control cells)×100].

2.3.2 Assessment of unstained cell morphological assay

Hep G2 cells were grown on glass cover slip (22×22 mm) placed in six well plates at a density of 5×10^5 cells/well and incubated for 24 h before treatment with the IC_{50} (50% Inhibitory concentration after treatment) values of compounds **17-24**. The medium was subsequently removed from each well of the sham control and the compounds treated Hep G2 cells after 24 h and/or 48 h incubation. The cover slips were then inverted and placed over micro slides. The gross morphological changes in the compounds treated and sham control cells were observed using a differential interference phase contrast light microscope (Axio Scope A1, Carl Zeiss, Jena, Germany) and photographed at 40X magnification.

2.3.3 Acridine Orange /Ethidium bromide double staining

To characterize the cell apoptosis as a result of the synthesized compounds, Acridine Orange (AO)/Ethidium bromide (EB) staining was performed to detect the apoptotic cell morphology as described by Spector et al.[50] Equal volumes of AO (100µg/mL) and EB (100µg/mL) in phosphate-buffered saline (PBS) were prepared for staining. Cells (Hep G2) were grown on glass cover slips in six well plates (5×10^5 cells/well) for 24h. The cells were then incubated with the IC_{50} dose of all newly synthesized compounds **17-24** for 24 h. After incubation the medium was discarded and the cells were washed with PBS. The cells were then trypsinized, placed on a glass slide, stained with AO/EB and examined using a fluorescent microscope with an UV filter (450-490 nm). The cells reflecting pathological changes were observed, calculated and photographed at 40X magnification (Axio Scope A1, Carl Zeiss, Jena, Germany).

2.4. Instrumentation

The melting points were determined in open capillary tubes and are uncorrected. Infra–red spectra were recorded on Thermo Nicolet FT–IR model *i*S5 spectrophotometer using KBr pellet. The NMR spectra were recorded at 400 MHz and 300 MHz Bruker instruments using Tetramethylsilane (TMS) as an internal standard. Deuterated chloroform/deuterated DMSO was used to record all NMR spectra and the chemical shifts are reported in δ units (parts per million) relative to the standard. Mass spectra were recorded on VG7070H and Thermo Nicolet Exactive Plus mass spectrometers. All reactions were monitored by thin layer chromatography using silica gel precoated aluminium sheets of Merck TLC 60 F254 and visualized in UV light chamber. All reactions were carried out using analytical grade solvents without further purification.

2.5. Synthetic Procedures

2.5.1 General procedure for the preparation of compounds 1–8

Mannich condensation of appropriate ketones, aldehydes and ammonium acetate or methyl amine in the ratio of 1:2:1 respectively, in the medium of 95% ethanol gives substituted 3–alkyl–2,6–diarylpiperidin–4–ones. The crude product was obtained after acid/base workup and recrystallised by slow evaporation method in ethanol gives pure compound.

2.5.2 General procedure for the preparation of compounds 9-16

To the completely dissolved solution of substituted 3–alkyl–2,6–diphenylpiperidin–4–one (1.0 mmol) in methanol, 0.2 mL of conc. HCl and methanolic solution of thiosemicarbazide (1.0 mmol) was added dropwise with stirring. The reaction mixture was refluxed with water condenser for 2 h. After completion, the reaction mixture was cooled to room temperature and the solid separated was filtered. The crude product was recrystallised from methanol.

2.5.3 General procedure for the synthesis of compounds 17–24

To a warm solution of substituted 3–alkyl–2,6–diarylpiperidin–4–one thiosemicarbazones (1.0 mmol) in methanol, methanolic solution of DMAD (1.0 mmol) /DEAD (1.0 mmol) was added drop wise with stirring. The reaction mixture was allowed to stirred at 60°C for 2 h. The completion of reaction was confirmed by TLC and the reaction mixture was cooled to room temperature. The yellow solid obtained was filtered and washed with warm methanol.

(*E*)-methyl 2-(2-(1,3-dimethyl-2,6-diphenylpiperidin-4-ylidene)hydrazinyl)-4-oxo-4H-1,3-thiazine-6-carboxylate (**17**).

Pale yellow powder, yield: 87%. M.p. 183-185 °C; ^{1}H NMR (400 MHz, $CDCl_3$, δ ppm) 0.87 (d, 3H), 1.69 (s, 3H), 2.37 (t, 1H), 2.75 (m, 1H), 2.90 (d, 1H), 3.22 (d, 1H), 3.53 (d, 1H), 3.85 (s, 3H), 6.86 (s, 1H), 7.44 – 7.26 (m, 10H). ^{13}C NMR (125 MHz, $CDCl_3$) δ: 12.81, 38.61, 41.47, 45.57, 52.57, 69.94, 77.90, 116.08, 127.21−128.69, 142.40, 142.90, 144.16, 157.47, 165.44, 166.44, 171.10. HRMS (ESI/$(M+H)^+$) calcd for $C_{25}H_{26}N_4O_3S$ 463.1805 found 463.1821.

(*E*)-methyl 2-(2-(2,6-bis(4-methoxyphenyl)-3-methylpiperidin-4-ylidene)hydrazinyl)-4-oxo-4H-1,3-thiazine-6-carboxylate (18).

Pale yellow powder, yield: 76%. M.p. 211-213 °C; ^{1}H NMR (400 MHz, DMSO-d_6, δ ppm) 0.92 (d, 3H), 3.17 (t, 1H), 3.57 (m, 1H), 3.71 (s, 1H), 3.77 (s, 3H), 3.79 (s, 6H), 4.35 (d, 1H), 4.58 (d, 1H), 6.68 (s, 1H), 7.74 – 6.98 (m, 8H). ^{13}C NMR (125 MHz, DMSO-d_6) δ: 11.87, 31.92, 40.19, 52.44, 55.19, 58.79, 65.51, 114.44, 126.80−130.39, 142.83, 160.41, 165.60, 165.68, 165.89. HRMS (ESI/$(M+H)^+$) calcd for $C_{26}H_{28}N_4O_5S$ 509.1859 found 509.1895.

(*E*)-ethyl-2-(2-(1,3-dimethyl-2,6-diphenylpiperidin-4-ylidene)hydrazinyl)-4-oxo-4H-1,3-thiazine-6-carboxylate (19).

Pale yellow powder, yield: 83%. M.p. 196-198 °C; ^{1}H NMR (400 MHz, $CDCl_3$, δ ppm) 0.87 (d, 3H), 1.34 (t, 3H), 1.70 (s, 3H), 2.36 (s, 1H), 2.76 (s, 1H), 2.89 (s, 1H), 3.22 (s, 1H), 3.53 (d, 1H), 4.30 (q, 2H), 6.85 (s, 1H), 7.41 – 7.26 (m, 10H). ^{13}C NMR (125 MHz, $CDCl_3$) δ: 12.78, 14.17, 38.56, 41.42, 45.51, 61.68, 69.91, 77.89, 116.59, 127.21−128.66, 142.04, 157.80, 165.62, 165.94, 170.90. $C_{26}H_{28}N_4O_3S$, MS: 477.195 ($[M+H]^+$).

(*E*)-methyl 2-(2-(2,6-bis(4-chlorophenyl)-3-methylpiperidin-4-ylidene)hydrazinyl)-4-oxo-4H-1,3-thiazine-6-carboxylate (20).

Yellow powder, yield: 82%. M.p. 205-207 °C; ^{1}H NMR (300 MHz, DMSO-d_6, δ ppm) 0.93 (d, 3H), 3.21 (t, 1H), 3.63 (m, 1H), 3.72 (d, 1H), 3.77 (s, 3H), 4.46 (d, 1H), 4.69 (d, 1H), 6.68 (s, 1H), 7.90 – 7.52 (m, 8H). ^{13}C NMR (100 MHz, DMSO-d_6) δ: 11.75, 31.84, 52.36, 58.73, 65.34, 114.42, 128.51−134.63, 142.78, 160.55, 164.92, 165.57, 165.79. $C_{24}H_{22}Cl_2N_4O_3S$, MS: 517.086 ($[M+H]^+$).

(*E*)-ethyl 2-(2-(2,6-bis(4-chlorophenyl)-3-methylpiperidin-4-ylidene)hydrazinyl)-4-oxo-4H-1,3-thiazine-6-carboxylate (21).

Yellow powder, yield: 78%. M.p. 217-219 °C; ^{1}H NMR (300 MHz, DMSO-d_6, δ ppm) 0.93 (d, 3H), 1.25 (t, 3H), 3.17 (t, 1H), 3.60 (m, 1H), 3.76 (d, 1H), 4.23 (q, 2H), 4.45 (d, 1H), 4.68 (d, 1H), 6.65 (s, 1H), 7.88 – 7.52 (m, 8H). ^{13}C NMR (100 MHz, DMSO-d_6) δ: 11.79, 13.95, 31.89, 58.81, 61.31, 65.40, 114.75, 128.55–134.72, 142.69, 160.72, 164.91, 165.33, 165.64. $C_{25}H_{24}Cl_2N_4O_3S$, MS: 531.101 ([M+H]$^+$).

(*E*)-methyl 2-(2-(2,6-bis(4-chlorophenyl)-3-ethylpiperidin-4-ylidene)hydrazinyl)-4-oxo-4H-1,3-thiazine-6-carboxylate (22).

Yellow powder, yield: 77%. M.p. 227-229 °C; ^{1}H NMR (300 MHz, DMSO-d_6, δ ppm) 0.91 (t, 3H), 1.46 (q, 2H), 3.16 (t, 1H), 3.60 (s, 1H), 3.74 (s, 3H), 4.60 (m, 1H), 4.71 (m, 1H), 6.69 (s, 1H), 7.90 – 7.52 (m, 8H). ^{13}C NMR (100 MHz, DMSO-d_6) δ: 10.31, 18.46, 32.04, 45.22, 52.37, 58.69, 63.58, 114.41, 128.46–138.68, 142.85, 160.48, 163.59, 165.56, 165.78. $C_{25}H_{24}Cl_2N_4O_3S$, MS: 531.101 ([M+H]$^+$).

(*E*)-ethyl 2-(2-(2,6-bis(4-chlorophenyl)-3-ethylpiperidin-4-ylidene)hydrazinyl)-4-oxo-4H-1,3-thiazine-6-carboxylate (23).

Yellow powder, yield: 74%. M.p. 232-234 °C; ^{1}H NMR (300 MHz, DMSO-d_6, δ ppm) 0.91 (t, 3H), 1.25 (t, 3H), 1.47 (m, 2H), 3.77 (d, 1H), 4.23 (q, 2H), 4.59 (s, 1H), 4.69 (d, 1H), 6.65 (s, 1H), 7.84 – 7.52 (m, 8H). ^{13}C NMR (100 MHz, DMSO-d_6) δ: 10.33, 13.89, 18.47, 32.04, 45.26, 58.65, 61.26, 63.57, 114.78, 128.48–134.70, 142.60, 160.32, 163.55, 165.20, 165.59. $C_{28}H_{32}Cl_2N_4O_3S$, MS: 545.117 ([M+H]$^+$).

(*E*)-methyl 2-(2-(3-isopropyl-2,6-diphenylpiperidin-4-ylidene)hydrazinyl)-4-oxo-4H-1,3-thiazine-6-carboxylate (24).

Pale yellow powder, yield: 85%. M.p. 201-203 °C; ^{1}H NMR (400 MHz, DMSO-d_6, δ ppm) 0.98 (d, 3H), 1.113 (d, 3H), 1.672 (s, 2H), 2.30 (t, 1H), 2.68 (d, 1H), 3.61 (d, 1H), 3.76 (s, 3H), 3.93 (d, 1H), 3.98 (d, 1H), 6.62 (s, 1H), 7.53 – 7.26 (m, 10H). ^{13}C NMR (125 MHz, DMSO-d_6) δ: 17.42, 20.82, 26.93, 31.53, 52.31, 54.09, 59.75, 64.86, 113.39, 126.62–128.24, 142.60, 165.98, 166.47. $C_{26}H_{28}N_4O_3S$, MS: 477.195 ([M+H]$^+$).

3. Results and Discussions

3.1. Reaction Mechanism

The first step of the mechanism involves the conjugate addition of sulfur atom onto the triple bond of the acetylene and the resulting intermediate undergoes intra–molecular condensation *via* aminolysis of the ester group followed by the elimination of an alcohol molecule. The cyclization of this intermediate has been claimed for two different structures, either i) α–cyclization resulting in the formation of a six–membered thiazin–4–one ring or ii) β–cyclization resulting in the formation of a five–membered thiazolidin–4–one ring (**Fig. 1**). It has been observed from the spectral analysis that the intermediate is actually participated in α–cyclization leading to the formation of six–membered thiazin–4–ones regioselectively (**Scheme 1**).[51-53]

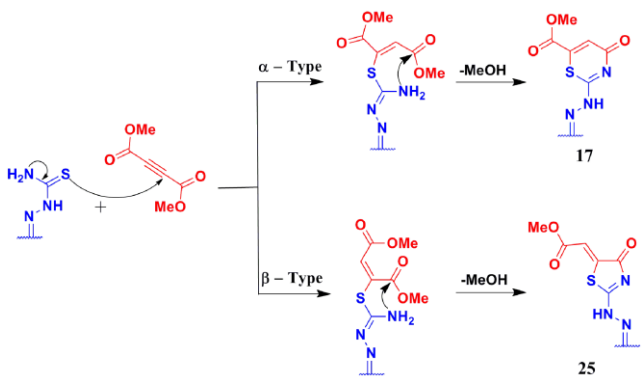

Fig. 1 Plausible mechanism of the reaction between thioamide and DMAD.

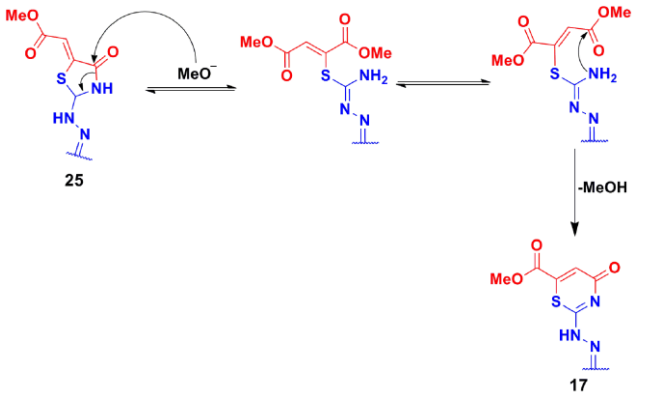

Fig. 2 Formation of six membered thiazinone from the unstable five membered thiazolidinone

On the other hand, there is a possibility of thiazinone formation by the attack of methoxide ion on cyclic amide carbonyl, leading to the unstable thiazolidinone ring which will undergo a ring opening and consequent ring closure involving the other ester carbonyl to give the six membered thiazinone[54,55] as the final product (**Fig. 2**).

3.2. Spectral Analyses

The structure of newly synthesized compounds was supported by spectral analyses such as FT–IR, HR–Mass, 1D and 2D NMR spectra. The numbering pattern followed for compounds **17–24** to explain the spectra was given in **Fig. 3.** The ^{1}H NMR spectrum splitting patterns are noted as broad singlet (bs), singlet (s), doublet (d), triplet (t), quintet (q) and multiplet (m). Compound **17** was considered as a representative for the synthesized compounds and the 2D NMR spectra were recorded for it to elucidate the structure.

3.2.1 FT–IR and HR–Mass spectral analyses

FT–IR spectrum (Fig. S1) recorded for the representative compound **17** exhibits four sharp intense bands at 1733, 1702, 1642 and 1618 cm^{-1} characteristics of ester carbonyl, amide carbonyl and imino group of thiazinone ring and imino group of piperidine respectively, whereas the *–NH–* in 9th position showed a broad band at 3389 cm^{-1}. Mass spectra were recorded for the new compounds and the observed peaks with mass values (M+H)$^+$ confirmed the formation of the products.

3.2.2 ^{1}H, ^{13}C and 2D NMR spectral analyses of the compound 17

In the ^{1}H NMR (Fig. S2) spectrum, a sharp singlet at **1.69** ppm with three protons integral corresponds to methyl protons H–7a attached to the piperidones ring nitrogen. A doublet at **0.87** ppm is corresponding to methyl protons H–3'a attached to carbon 3 and it shows HOMO correlation with the multiplet signal at **2.75** ppm obviously due to H–3a proton in ^{1}H–^{1}H

View Article Online
DOI: 10.1039/C5NJ01768K

COSY spectrum (Fig. S5). Moreover, the methoxy protons H–h in the ester group of compound **17** resonate as a sharp singlet at **3.85** ppm. The aromatic proton signals of two phenyl rings of the compound **17** appear in the region of **7.44** to **7.27** ppm as multiplet. A sharp singlet appeared at **6.86** ppm with one proton integral was assigned to methine proton H–e present in the thiazinone ring. For compound **17**, one of the two benzylic protons appears as a doublet at **3.22** ppm is assigned for H–6a proton and the other doublet at **2.90** ppm is assigned for H–2a proton as the later has correlation with H–3a in ^{1}H–^{1}H COSY. The doublet at **3.53** ppm with one proton integral corresponding to H–5e proton is confirmed by ^{1}H–^{1}H correlation with H–6a proton (3.22 ppm). A triplet appeared at **2.37** ppm with one proton integral corresponding to H–5a proton is confirmed by HOMO correlation with H–6a (3.22 ppm) and H–5e (3.53 ppm). The large coupling constants were observed between H2 & H3 protons (J = 10.0 Hz) and H5 & H6 protons (J = 10.8 Hz) which suggested that the piperidone ring exist largely in normal chair conformation with equatorial orientation of C–3 methyl and aryl groups.

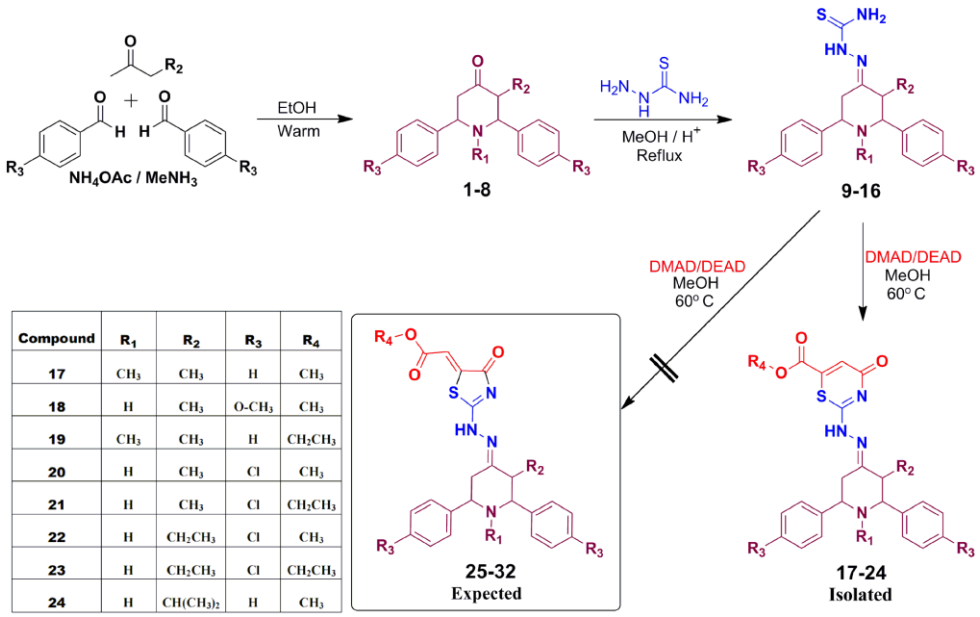

Compound	R_1	R_2	R_3	R_4
17	CH_3	CH_3	H	CH_3
18	H	CH_3	O-CH_3	CH_3
19	CH_3	CH_3	H	CH_2CH_3
20	H	CH_3	Cl	CH_3
21	H	CH_3	Cl	CH_2CH_3
22	H	CH_2CH_3	Cl	CH_3
23	H	CH_2CH_3	Cl	CH_2CH_3
24	H	$CH(CH_3)_2$	H	CH_3

Scheme 1. The reaction between 3–alkyl–2,6–diarylpiperidin–4–one thiosemicarbazones and acetylene diesters.

Table 1. ^{1}H–^{1}H COSY, ^{1}H–^{13}C COSY and HMBC correlations of compound **17**

^{1}H Chemical shifts (ppm)	Correlations (ppm)		
	^{1}H–^{1}H COSY	^{1}H–^{13}C COSY	HMBC
0.87 (d, 3H, H–3'a)	2.75 (m)	12.81	77.90, 45.57, 12.81, 171.10
1.69 (s, 3H, H–7a)	———	41.47	77.90, 69.94
2.37 (t, 1H, H–5a)	3.53 (d), 3.22 (d)	38.61	69.94, 171.10, 144.16
2.75 (m, 1H, H–3a)	2.90 (d), 0.87 (d)	45.57	12.81, 171.10, 77.90
2.90 (d, 1H, H–2a)	2.75 (m)	77.90	69.94, 45.57, 41.47, 12.81, 128.69, 142.90
3.22 (d, 1H, H–6a)	3.53 (d), 2.37 (t)	69.94	127.21
3.53 (d, 1H, H–5e)	3.22 (d), 2.37 (t)	38.61	45.57, 171.10
3.85 (s, 3H, H–h)	———	52.57	166.44
6.86 (s, 1H, H–e)	———	116.08	116.08, 165.44, 142.40
7.44 – 7.26 (m)	———	128.69 – 127.21	77.90, 69.94, 127.21 – 128.69, 142.90, 144.16

In ^{13}C NMR spectrum (Fig. S3), the signals at **77.9**, **69.9**, **45.5** and **38.6** ppm in the aliphatic region are assigned to C–2, C–6, C–3 and C–5 carbons of the piperidine ring based on one bond correlations with H–2a (2.90 ppm) H–6a (3.22 ppm) and H–3a (2.75 ppm) in the ^{1}H–^{13}C COSY spectrum (Fig. S6) and the negative peak observed at **38.5** ppm in the DEPT-135 spectrum

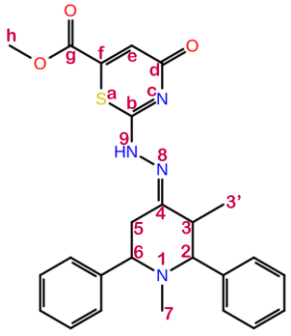

Fig. 3 Numbering pattern of compound **17** followed for the spectral explanations.

(Fig. S4) for C–5 carbon. The 2D NMR correlations of compound **17** are given in **Table 1**. The methylene carbon C–5 is also confirmed in ^{1}H–^{13}C COSY by its cross peak with H–5a (2.37 ppm) and H–5e (3.53 ppm). The signal at **41.4** ppm is assigned to C–7 carbon as observed by the one bond correlation with H–7a (1.69ppm) in ^{1}H–^{13}C COSY and multiple bond correlation with H–2a (2.90 ppm) in HMBC spectrum (Fig. S7). The signal at **12.8** ppm in the HMBC is assigned to methyl

[Type text]

carbon C–3' attached to the C–3 as it shows cross peak with H–3'a (0.87 ppm) and α correlation with H–3a (2.75 ppm) and β correlation with H–2a (2.90 ppm). Moreover, the signal at **52.5** ppm is assigned to methyl carbon C–h of the ester group is as evidenced by one bond correlation with the corresponding methyl protons H–h (3.85ppm).The signal nearer to aromatic region at **116.0** ppm has one bond correlation with methine proton H–e present in the thiazinone ring (6.86ppm) and it is assigned for C–e carbon. The signal at **171.1** ppm shows multiple bond correlation with **2.37** ppm (H–5a), **3.53** ppm (H–5e), and also with **2.75** ppm (H–3a), **0.87** ppm (H–3'a) in the HMBC spectrum is assigned for C–4 carbon. The quaternary carbon signal at **142.4** ppm shows HMBC correlation with H–e (6.86 ppm) and it is assigned for C–f carbon. The less intense quaternary carbon signal at **157.4** ppm is assigned for C–b carbon.

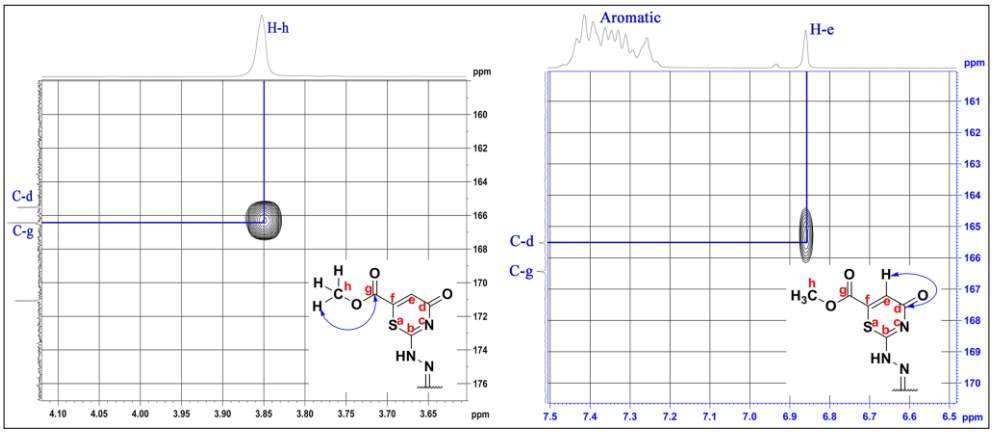

Fig. 4 The expansions of HMBC spectrum of compound **17**.

Table 2. LUMO-HOMO energy gap of compounds **17** and **25**.

Level of Theories / basis set	LUMO-HOMO energy gap of 17 (eV)	LUMO-HOMO energy gap of 25 (eV)	Energy difference between 17 and 25 (eV)
B3LYP/6–31G**	4.05590	4.03328	0.02262
B3LYP/6–311G**	4.07044	4.04345	0.02699
M06/6–31G**	4.66615	4.64301	0.02314
M06/6–311G**	4.72981	4.65577	0.07404
M06/6–311G–3DF–3PD	7.47820	7.42291	0.05529

The expansions of HMBC spectrum were displayed in **Fig. 4**. The ^{13}C signal at **166.4** ppm is assigned for the ester carbonyl group C–g based on the β–correlation with the proton at **3.85** ppm (H–h). The signal of C–g (166.4 ppm) does not show any other correlation with the proton peak at **6.86** ppm (H–e), whereas the signal at **165.44** is assigned to amido carbonyl carbon C–d shows α–correlation with the proton signal at **6.86** ppm (H–e). Therefore, these observations unequivocally confirm the cyclization of acetylenes with 3–alkyl–2,6–diarylpiperidin–4–one thiosemicarbazone derivatives to give six–membered thiazin–4–ones and hence the formation of compounds **25–32** was ruled out.

3.3. Computational Results

In HOMO and LUMO calculations, the results obtained using all the levels of theories indicated that the energy gap of the compound **17** with thiazinone ring were slightly higher than the compound **25** with thiazolidinone ring and hence compound **17** was considered as a stable form for the representative compound. The energy gap values of compounds **17** and **25** are given in **Table 2**. The pictorial representation of HOMO and LUMO of all levels is given in the supplementary data (Table S1).

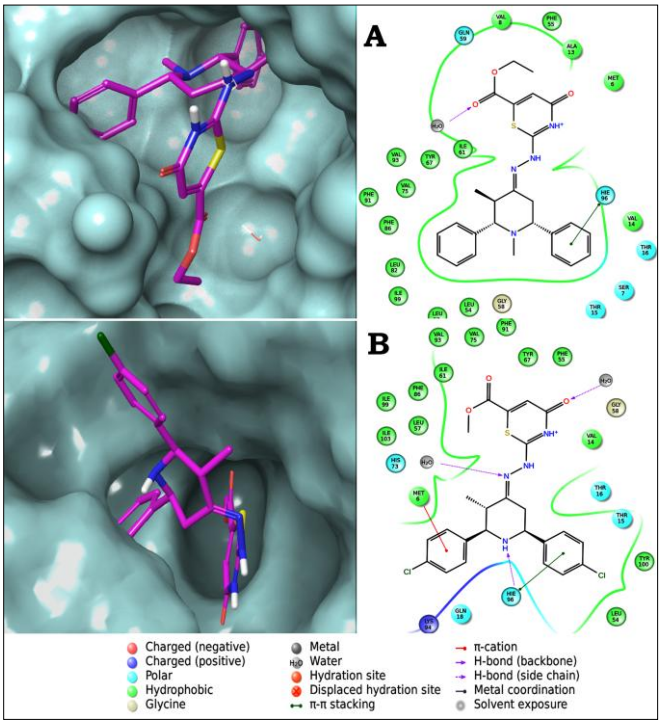

Fig. 5 Docking poses of A) Compound 19 and B) Compound 20 with MDM2 protein, PDB ID: 4ODE.

The *Lipinski's rule of five* values of compounds **17–24** indicate that the compounds are endowed with drug like properties. Compounds **17**, **19**, and **24** showed no violation on *Lipinski's rule of five*. All other compounds (**18**, **20**, **21**, and **22**) showed one violation except compound **23**, which showed 2 violations owing to its partition coefficient value between octanol and water is more than 5 and the molecular weight is greater than

500 amu. The drug–like prediction results by *Qikprop* are tabulated in **Table 3**. The tested compounds have satisfactory percentage of human oral absorption except compounds **18** and **23** which have less than 70%. Predicted aqueous solubility (QPlogS) parameter indicated that the compounds **17**, **18**, **19** and **24** possess permissible values and the chloro substituted compounds (**20**, **21**, **22**, and **23**) are having poor aqueous solubility. The prediction of blood brain barrier permeability (QPlogBB) for the tested compounds was assessed and all the compounds were predicted to have acceptable values. The IC_{50} value of HERG K+ channel blockage (QPlogHERG) was also predicted and the results showed that all the tested compounds have moderate range of values.

Table 3. Pharmacokinetic properties of compounds **17–24**

Comp	Factors of Lipinski's rule of five					Pharmacokinetic properties			
	mol_MW (< 500)	Donor HB (< 5)	Accpt HB (< 10)	QPlogPo/w (< 5)	Rule of Five	Percent Human Oral Absorption[a] (> 80 high, < 25 poor)	QPlogS[b] (–6.5 to 0.5)	QPlogHERG[c] (below –5)	QPlogBB[d] (–3 to 1.2)
17	462.565	1	9	3.375	0	77.765	–5.717	–7.816	–1.186
18	508.591	2	10	3.525	1	66.254	–6.263	–7.713	–1.379
19	476.592	1	9	3.817	0	81.491	–6.241	–8.043	–1.242
20	517.429	2	8.5	4.451	1	70.759	–7.860	–7.935	–1.042
21	531.456	2	8.5	4.660	1	73.580	–7.627	–7.768	–0.930
22	531.456	2	8.5	4.647	1	73.520	–7.451	–7.752	–0.923
23	545.482	2	8.5	5.022	2	63.080	–7.915	–7.906	–1.021
24	476.592	2	8.5	4.009	0	86.528	–6.148	–7.869	–0.894

[a]Percentage of human absorption, [b]Predicted aqueous solubility; S in mol/L, [c]Predicted IC_{50} value for blockage of HERG K+ channels, [d]Predicted blood brain barrier permeability

Docking studies was carried out to evaluate the binding affinity and the interactions between the synthesized compounds and the MDM2 protein (PDB ID: 4ODE). The docking score of the compounds **17-24** varies from -8.427 to -7.027. The *evdw* and *ecoul* are the predicted van der Waals' interaction and electrostatic interaction energies between ligand and the protein.

Table 4. Docking results of compounds **17-24** with MDM2 protein (PDB ID: 4ODE)

Entry	Comp.	XP GScore	Glide evdw	Glide ecoul	Interacting Residues
1	**17**	-8.046	-39.835	2.373	H_2O 326
2	**18**	-7.238	-42.618	-3.552	GLN 59, H_2O 312
3	**19**	-7.88	-19.387	5.124	HIE 96, H_2O 312
4	**20**	-7.531	-46.244	-5.198	HIE 96, MET 6, H_2O 312 & H_2O 338
5	**21**	-7.48	-43.657	0.881	H_2O 326
6	**22**	-7.057	-38.596	1.12	H_2O 338
7	**23**	-7.027	-44.717	-1.989	TYR 67
8	**24**	-8.427	-35.388	-2.565	H_2O 312

The docking results clearly indicate that the water molecules present in the active site of MDM2 protein plays an important role in binding. All the tested compounds display interactions with one or two water molecules (Fig. S37). The interactions between 4ODE and the compounds are tabulated in **Table 4**. Compounds **17**, **19**, **20** and **24** have good glide score and the compounds **19** and **20** exhibited good interactions with an important residue *HIE 96* by π–π stacking which is essential for the inhibitory activity of MDM2.[56] These π–π stacking interactions were performed by the phenyl ring attached to the sixth position of the piperidyl ring. Compound **20** also showed π–cation interaction with *MET 6* and hydrogen bond interactions with two water molecules. The interactions between the MDM2 protein and the compounds **19** and **20** are shown in **Fig. 5**. The tested compounds **18** and **23** form hydrogen bond interactions with *GLN 59* and *TYR 67* respectively.

3.4. Antitumor Studies

3.4.1 Cytotoxicity Results

The cytotoxicity of the tested compounds **17-24** were evaluated against human Hep G2 cell line in various concentrations *viz.* 10 µM, 20 µM, 30 µM, 40 µM, 50 µM, 60 µM, 70 µM, 80 µM, 90 µM, and 100 µM. **Fig. 6** shows the inhibitory effect of the synthesized compounds **17-24** on Hep G2 liver cancer cells after 24 h and 48 h respectively.

Treated cells showed shrinkage in volume of cells, membrane blebbing and loss of cell adhesion. The IC_{50} values of the novel compounds ranges from 10 to 100 µM and tabulated in **Table 5**. The screening results revealed that the tested compounds exhibited good and moderate antitumor activity against Hep G2 cell line. Among this series, compounds **17** and **19** showed significant activity in the tested cells (**Fig. 7**) with IC_{50} values 33.05±0.95 and 49.82±0.61 µM for 24 h and 22.03±1.61 and 28.58±2.53 µM for 48 h respectively. It was observed that the *N-CH_3* piperidyl ring (compounds **17** and **19**) plays an important role in enhancing the cytotoxicity of these compounds. The compounds **20**, **21**, **22** and **23** with chloro

[Type text]

substitution pattern displayed moderate anticancer activity. Whereas the remaining compounds **18** and **24** showed

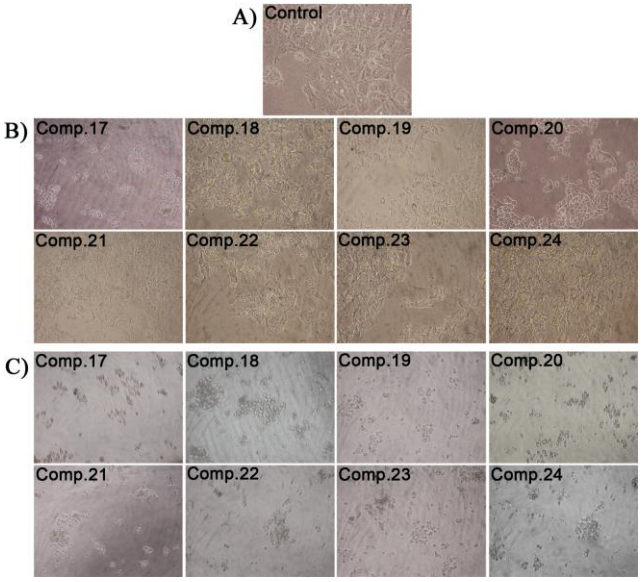

Fig. 6 Morphological observations of Hep G2 cells by inverted microscope at actual magnification 40X. **A)** Untreated control cells **B)** Hep G2 cell line showing nuclear fragmentation upon treatment with compounds **17-24** after 24 h, **C)** After 48 h.

lower anticancer potency as compared to other compounds. These aspects show that the methyl substitution (*N-CH*$_3$) in the piperidyl ring is important to enhance the anticancer activity.

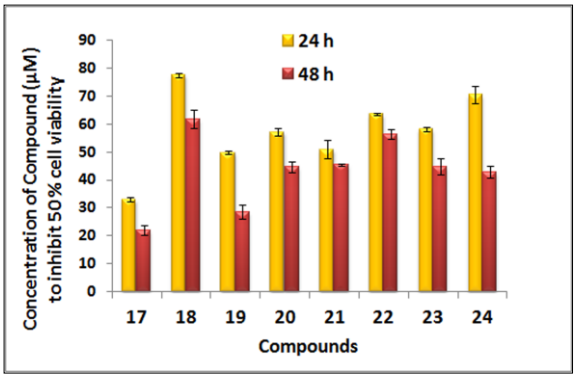

Fig. 7 IC_{50} range of Compounds **17-24** against Hep G2 human liver cancer cells. Data shown are the mean values from six independent experiments.

Table 5. IC_{50} values (expressed in μM) of compounds **17-24** against human liver cancer cell line Hep G2.

Entry	Comp.	IC_{50} (μM)	
		24h	48h
1	17	33.05 ± 0.95	22.03 ± 1.61
2	18	77.63 ± 0.76	61.80 ± 3.17
3	19	49.82 ± 0.61	28.58 ± 2.53
4	20	57.26 ± 1.32	44.57 ± 1.90
5	21	51.03 ± 3.31	45.32 ± 0.47
6	22	63.58 ± 0.57	56.32 ± 1.67
7	23	58.29 ± 0.79	44.82 ± 2.84
8	24	70.52 ± 3.22	42.87 ± 2.27

3.4.2 Evaluation of Apoptosis (AO/EB Staining)

Hep G2 cells treated with IC_{50} dose of the synthesized compounds revealed apoptotic characteristics such as lose of cytoplasmic membrane integrity there by uptake of ethidium bromide making the nucleus stain red. Whereas the untreated Hep G2 cells were stained green as a result of intercalation into the double stranded DNA.

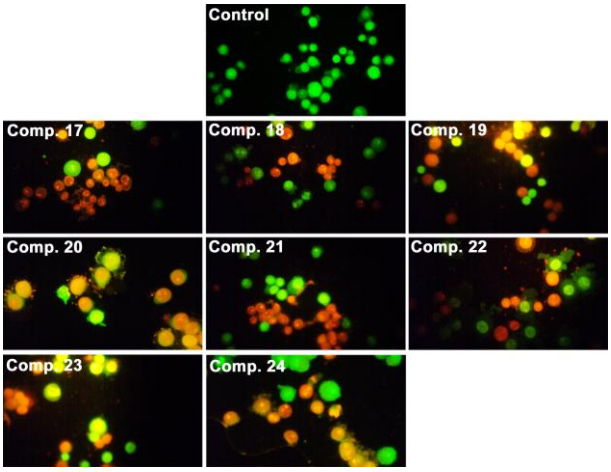

Fig. 8 Analysis of apoptotic characters of compounds **17-24** by AO/EB staining in liver carcinoma human cell line Hep G2 in fluorescence microscopy at 40X magnification.

Early apoptotic cells showed bright green nucleus with condensed or fragmented chromatin and late apoptotic cells display condensed and fragmented orange or red colored chromatin. Cells that have died from direct necrosis have a structurally normal orange nucleus. Analysis of apoptotic characters by AO/EB staining in Hep G2 cell line treated with newly synthesized compounds (**17-24**) using fluorescence microscopy is shown in **Fig. 8**. The treatment of compounds **17** and **19** caused more cells to undergo death in Hep G2 liver cancer cells, in agreement with the cytotoxic results. The observations revealed that all the compounds treated cells show cytological changes, whereas in the untreated cells, no such changes were observed. The photomicrographs in **Fig. 8** show viable (light green), early apoptotic (bright green), late apoptosis (red to orange) and necrosis (red) cells.

4. Conclusions

In conclusion, a convenient and efficient method to synthesize thiazin–4–one derivatives with good yields has been reported. The newly synthesized compounds were characterized by FT–IR, HR–Mass and 1D/2D NMR. All the spectral data unambiguously demonstrates the cyclization of DMAD or DEAD with 3–alkyl–2,6–diarylpiperdin–4–one thiosemicarbazone derivatives resulting in six–membered thiazin–4–one regioselectively. From the chemical shifts and coupling constants, the title compounds were found to adopt chair conformations with equatorial orientation of aryl groups. The representative compound (**17**) was theoretically studied using DFT at B3LYP and M06 level of theories and found to be in good agreement with the structure elucidated by 2D NMR

spectra. The interactions between the synthesized compounds and the tumor protein MDM2 were studied by molecular docking. The docking results indicate that the compounds **19** and **20** show interactions with the critical amino acid *HIE 96* which is necessary for the inhibition of MDM2 protein. The drug–like properties predictions show that the compounds **17**, **19** and **24** have no violations owing to the *Lipinski's rule of five* and other tested parameters. Furthermore, in the evaluation of antitumor studies, compounds **17** and **19** with *N-CH$_3$* substitution in the piperidyl ring showed good inhibitory activity against Hep G2 human liver cancer cell line. These compounds were also identified as a best molecules in drug–like properties prediction. The evaluation of apoptosis using AO/EB staining shows changes in the nuclear morphology by the formation of apoptotic bodies and these cell death also in agreement with the cytotoxicity results.

Acknowledgements

We gratefully acknowledge the funding support from University Grants Commission (UGC) Grant No. 39–689–2010 SR and Department of Biotechnology (DBT) Grant No. BT/PR14062/MED/30/357/2010, New Delhi, India. The computations have been supported by Department of Biotechnology–North East Collaboration (DBT–NEC) Research Project, Grant No. BT/252/NE/TBP/2011, New Delhi, India.

References

1 A. M. Clark, *Pharm. Res.,* 1996, **13**, 1133–1141.
2 C. J. Sutherland, J. E. Montgomery and I. G. Kestin, *Paediatr Anaesth.,* 1998, **8**, 321–324.
3 F. H. Shaw and A. Shulman, *Nature,* 1955, **175**, 388–389.
4 P. G. Lawlor, K. S. Turner, J. Hanson and E. D. Bruera, *Cancer,* 1998, **82,** 1167–1173.
5 M. Koch, K. Perumal, O. Blacque, J. A. Garg, R. Saiganesh, S. Kabilan, K. K. Balasubramanian and K. Venkatesan, *Angew. Chem.,* 2014, **126**, 6496-6500.
6 K. Narayanan, M. Shanmugam, G. Vasuki and S. Kabilan, *J. Mol. Struct.,* 2014, **1056–1057**, 70–78.
7 S. Umamatheswari, B. Balaji, M. Ramanathan and S. Kabilan, *Eur. J. Med. Chem.,* 2011, **46**, 1415–1424.
8 P. Karthikeyan, A. Meena Rani, R. Saiganesh, K.K. Balasubramanian and S. Kabilan, *Tetrahedron,* 2009 **65**, 811–821.
9 K. Narayanan, M. Shanmugam, S. Jothivel and S. Kabilan, *Bioorg. Med. Chem. Lett.,* 2012, **22**, 6602–6607.
10 S. Umamatheswari, B. Balaji, M. Ramanathan and S. Kabilan, *Bioorg. Med. Chem. Lett.,* 2010, **20**, 6909–6914.
11 R. Ramachandran, M. Rani, S. Senthan, Y. T. Jeong and S. Kabilan. *Eur. J. Med. Chem.,* 2011, **46**, 1926–1934.
12 S. Balasubramanian, C. Ramalingan, G. Aridoss and S. Kabilan, *Eur. J. Med. Chem.,* 2005, **40**, 694–700.
13 G. Aridoss, P. Parthiban, R. Ramachandran, M. Prakash, Y. T. Jeong and S. Kabilan, *Eur. J. Med. Chem.,* 2009, **44**, 577– 592.
14 G. Aridoss, S. Balasubramanian, P. Parthiban and S. Kabilan, *Eur. J. Med. Chem.,* 2007, **42**, 851–860.
15 S. Balasubramanian, G. Aridoss, P. Parthiban, C. Ramalingan and S. Kabilan, *Biol. Pharm. Bull.,* 2006, **29**, 125–130.
16 G. C. Nandi, S. Samai and M. S. Singh, *J. Org. Chem.,* 2011, **76**, 8009–8014.
17 A. A. Esmaeili, A. Moradi and H. K. Mohammadi, *Tetrahedron,* 2010, **66**, 3575–3578.
18 V. Nair, A. Deepthi, M. Poonoth, B. Santhamma, S. Vellalath, B. P. Babu, R. Mohan and E. Suresh, *J. Org. Chem.,* 2006, **71**, 2313–2319.
19 M. Fan, Z. Yan, W. Liu and Y. Liang, *J. Org. Chem.,* 2005, **70**, 8204–8207.
20 M. G. Bhovi and G. S. Gadaginamath, *Indian J. Chem.*, 2005, **44B,** 1068–1073.
21 *Maestro*, version 9.3.5, Schrödinger, LLC, New York, 2012.
22 Y. Rew, D. Sun, F. G. D. Turiso, M. D. Barberger, H. P. Beck, J. Canon, A. Chen, D. Chow, J. Diegnan, B. M. Fox, D. Gustin, X. Huang, M. Jlang, X. Jiao, L. Jin, F. Kayser, D. J. Kopecky, Y. Li, M. Lo, A. M. Long, K. Michelsen, J. D. Oliner, T. Osgood, M. Ragains, A. Y. Saiki, S. Schneider, M. Toteva, P. Yakowec, X. Yan, Q. Ye, D. Yu, X. Zhao, J. Zhou, J. C. Medina and S. H. Olson, *J. Med. Chem.,* 2012, **55,** 4936-4954.
23 N. A. Danilkina, L. E. Mikhailov and B. A. Ivin, *Russ. J. Org. Chem*., 2006, **42**, 783-814.
24 I. Yavari, M. Sabbaghan, K. Porshamsian, M. Bagheri, S. A. Asgari and Z. Hossaini, *Mol. Divers,* 2007, **11,** 81–85.
25 V. S. Berseneva, A. V. Tkachev, Y. Y. Morzherin, W. Dehaen, I. Luyten, S. Toppet and V. A. Bakulev, *J. Chem. Soc. Perkin Trans.,* 1998, **1,** 2133–2136.
26 G. N. Lipunova, E. V. Nosova, A. A. Laeva, T. V. Trashakhova, P. A. Slepukhin and V. N. Charushin, *Russ. J. Org. Chem.,* 2008, **44,** 741–749.
27 J. J. Wade, *J. Org. Chem.,* 1979, **44**, 1816–1819.
28 V. A. Bakulev, V. S. Berseneva, N. P. Belskaia, Y. Y. Morzherin, A. Zaitsev, W. Dehaen, I. Luyten and S. Toppet, *Org. Biomol. Chem.,* 2003, **1,** 134–139.
29 (a)V. P. M. Rahman, S. Mukhtar, W.H. Ansari and G. Lemiere, *Eur. J. Med. Chem.,* 2005, **40**, 173–184;
(b) D. Havrylyuk, B. Zimenkovsky, O. Vasylenko, C.W. Day, D. F Smee, P. Grellier and R. Lesyk, *Eur. J. Med. Chem.,* 2013, **66,** 228–237;
(c) H. Zhou, S. Wu, S. Zhai, A. Liu, Y. Sun, R. Li, Y. Zhang, S. Ekins, P. W. Swaan, B. Fang, B. Zhang and B. Yan, *J. Med. Chem.,* 2008, **51,** 1242–1251.
30 (a) K. Mogilaiah, P. R. Reddy and R. B. Rao, *Indian J. Chem.,* 1999, **38B,** 495–500;
(b) D. Patel, P. Kumari and N. Patel, *Eur. J. Med. Chem.,* 2012, **48,** 354–362.
31 (a) H. Yamashita, K. Ohno, H. Inami, J. Shishikura, S. Sakamoto, M. Okada and T. Yamaguchi, *Eur. J. Pharmacol.,* 2004, **494,** 147–154;
(b) C. Dwivedi, T. K. Gupta and S. S. Parmar, *J. Med. Chem.,* 1972, **15**, 553–554.
32 (a) B. A. Sobin, *J. Am. Chem. Soc.,* 1952, **74,** 2947–2948;
(b) A. S. Narute, P. B. Khedekar and K. P. Bhusari, *Indian J. Chem.,* 2008, **47B**, 586–591.
33 M. L. Barreca, J. Balzarini, A. Chimirri, E. D. Clercq, L. D. Luca, H. D. Holtje, M. Holtje, A. M. Monforte, P. Monforte, C. Pannecouque, A. Rao and M. Zappalà, *J. Med. Chem.,* 2002, **45,** 5410–5413.
34 K. Ohno, R. Tsutsumi, N. Matsumoto, H. Yamashita, Y. Amada, J. Shishikura, H. I. S. Yatsugi, M. Okada, S. Sakamoto and T. Yamaguchi, *J. Pharmacol. Exp. Ther.,* 2003, **306,** 66–72.
35 C. J. Andres, J. J. Bronson, S. V. D'Andrea, M. S. Deshpande, P. J. Falk, K. A. Grant–Young, W. E. Harte, H. Ho, P. F. Misco, J. G. Robertson, D. Stock, Y. Sun and A. W. Walsh, *Bioorg. Med. Chem. Lett.,* 2000, **10,** 715–717.
36 C. R. Noller and V. Baliah, *J. Am. Chem. Soc.,* 1948, **70,** 3853–3855.
37 V. Baliah, R. Jeyaraman and L. Chandrasekaran, *Chem. Rev.,* 1983, **83,** 379–423.

[Type text]

View Article Online
DOI: 10.1039/C5NJ01369K

38 S. Balasubramanian, C. Ramalingam and S. Kabilan, *Indian J. Chem.,* 2002, **41B,** 2402–2404.
39 *Jaguar*, version 7.9, Schrödinger, LLC, New York, 2012.
40 *Qikprop*, version 3.5, Schrödinger, LLC, New York, 2012.
41 (a) C. A. Lipinski, F. Lombardo, B. W. Dominy and P. J. Feeney, *Adv. Drug Deliv. Rev.,* 1997, **23,** 3–25;
(b) C. A. Lipinski, F. Lombardo, B. W. Dominy and P. J. Feeney, *Adv. Drug Deliv. Rev.,* 2001, **46,** 3–26.
42 (a) P. Chene, *Nat. Rev. Cancer*, 2003, **3**, 102-109.
(b) K. Khoury, G. M. Popowicz, T. A. Holak and A. Domling, *Med. Chem. Commun.,* 2011, **2**, 246-260.
43 D. Bernard, Y. Zhao and S. Wang, *J. Med. Chem.,* 2012, **55**, 4934-4935.
44 A. Z. Gonzalez, Z. Li, H. P. Beck, J. Canon, A. Chen, D. Chow, J. Duquette, J. Eksterowicz, B. M. Fox, J. Fu, X. Huang, J. Houze, L. Jin, Y. Li, Y. Ling, M. Lo, A. M. Long, L. R. McGee, J. McIntosh, J. D. Oliner, T. Osgood, Y. Rew, A. Y. Saiki, P. Shaer, S. Wortman, P. Yakowec, X. Yan, Q. Ye, D. Yu, X. Zhao, J. Zhou, S. H. Olson, D. Sun and J. C. Medina, *J. Med. Chem.,* 2014, **57**, 2963-2988.
45 Protein Preparation Wizard; *Epik* version 2.3, 2012; *Impact* version 5.7, 2012, Schrödinger, LLC, New York.
46 W. L. Jorgensen, D. S. Maxwell and J. Tirado–Rives, *J. Am. Chem. Soc.,* 1996, **118**, 11225–11236.
47 *LigPrep*, version 2.5, 2012, Schrödinger, LLC, New York.
48 *Glide*, version 5.8, 2012, Schrödinger, LLC, New York.
49 T. Mosmann, *J. Immunol. Methods,* 1983, **65**, 55–63.
50 D. L. Spector, R. D. Goldman and L. A. Leinwand, Culture and biochemical Analysis of cells, In: Cell: A Laboratory Manual, 1998, 1, Cold Spring Harbor Laboratory Press, Cold Spring Harbor, New York.
51 N. A. Danilkina, L. E. Mikhaylov and B. A. Ivin, *Chem. Heterocycl. Compd.*, 2011**, 47**, 886−900.
52 B. Fabian, V. Kudar, A. Csampai, T. Z. Nagy and P. Sohar, *J. Organomet. Chem.,* 2007, **692**, 5621−5632.
53 N. Nami, M. Hosseinzadeh and E. Rahimi, *Phosphorus, Sulfur, and Silicon,* 2008, **183**, 2438−2442.
54 V. N. Britsun and M. O. Lozinskii, *Chem. Heterocycl. Compd*., 2007, **43**, 1083−1100.
55 R. M. Acheson and J. D. Wallis, *J. Chem. Soc. Perkin Trans. I*, 1981, 415−422
56 (a) F. Gonzalez-Lopez de Turiso, D. Sun, Y. Rew, M. D. Bartberger, H. P. Beck, J. Canon, A. Chen, D. Chow, T. L. Correll, X. Huang, L. D. Julian, F. Kayser, M. C. Lo, A. M. Long, D. McMinn, J. D. Oliner, T. Osgood, J. P. Powers, A. Y. Saiki, S. Schneider, P. Shaffer, S. H. Xiao, P. Yakowek, X. Yan, Q. Ye, D. Yu, X. Zhao, J. Zhou, J. C. Medina and S. H. Olson, *J. Med. Chem.,* 2013, **56**, 4053−4070.
(b) D. Bernard, Y. Zhao and S. Wang, *J. Med. Chem*., 2012, **55**, 4934−4935.